Effect of Bow-Type Initial Imperfection On Reliability of Minimum-Weight Stiffened Structural Panels

Effect of Bow-Type Initial Imperfection On Reliability of Minimum-Weight Stiffened Structural Panels

W. Jefferson Stroud
*Langley Research Center
Hampton, Virginia*

Thiagaraja Krishnamurthy and Nancy P. Sykes
Analytical Services and

Isaac Elishakoff
Florida Atlantic University

Contents

Summary

Computations were performed to determine the effect of an overall bow-type initial imperfection on the reliability of structural panels under combined compression and shear loadings. A panel's reliability is the probability that it will perform its intended function—in this case, carry a given load without buckling or exceeding in-plane strain allowables. For a panel loaded in compression, a small initial bow can cause large bending stresses that reduce both the buckling load and the load at which strain allowables are exceeded; hence, the bow reduces the reliability of the panel. In this report, analytical studies on two stiffened panels quantified that effect, which was found to be substantial.

Introduction

Numerous studies have shown that initial geometric imperfections can substantially reduce the load-carrying ability of thin plate and shell structures when the loading involves compression (e.g., refs. 1–6). Imperfections can have an even greater effect on these plate and shell structures if the structures are highly optimized without accounting for the imperfections. (Highly optimized structures can have substantial performance losses under any off-design condition.)

A smaller number of studies have used a probabilistic approach to relate the statistical nature of the imperfection (for example, its shape, magnitude, and distribution) to the probability that the structure can carry a given load. That probability is denoted the *reliability* of the structure. Many of these studies are cited and summarized in references 7–9.

The type of imperfection studied with a probabilistic approach in references 7–9 is a random nonsymmetric imperfection in circular cylindrical shell structures. Test data are used to obtain the statistics of the imperfections.

A different type of common initial geometric imperfection is an overall bow in a stiffened panel. An analysis procedure for calculating the effect of a bow on the stresses in and buckling loads of stiffened compression panels is described and demonstrated in references 10–15.

In this report, probabilistic concepts are combined with the analysis procedure of references 10–15. The objectives are (1) to establish the effect of a bow-type imperfection on the structural reliability of stiffened panels, (2) to assess the sensitivity of the reliability to accurate specification of the bow statistics, and (3) to illustrate the approach

used to compute the reliability. The size of the bow is the single random variable. The probability that a panel with this random bow can carry a specified load is the reliability of the panel at that load.

Two panels are considered. These panels are designed deterministically for minimum weight under the assumption that they are flat (i.e., without a bow). Both panels are blade-stiffened, made of graphite-epoxy, and designed for combined compression and shear loadings. However, one panel is designed to carry a greater load than the other.

First, the analysis-design procedure is summarized. Next, the design studies leading to the two minimum-weight panels are described. Then, the effect of a bow on the load-carrying ability of these two panels is discussed; failure mechanisms considered are buckling and excessive strain at the ply level. Finally, for various distributions of the bow, the reliability of the two panels is presented and discussed. Appendixes A–D contain additional explanations of the analysis-design procedure, tabulated values of failure load versus magnitude of the bow, example calculations, and information on the distribution functions and related statistical parameters for the distributions used in this report.

Symbols

A	area
b	depth of blade
c	distance from neutral surface of panel to location where strain is calculated
D_x	smeared orthotropic bending stiffness
E_1, E_2	Young's modulus of composite ply in fiber direction and transverse to fiber direction, respectively (table I)
ET	longitudinal extensional stiffness of panel
e	overall bow in panel, measured at panel midlength
e_i	values of e for a given value of F
$\bar{e}_i$	standardized values of e_i
$e_{\max}$	maximum allowable value of e
F	ratio of failure load to design load, defined in equation (A5)
F_s	specified value of F

G_{12}	in-plane shear modulus of composite ply in coordinate system defined by fiber direction (table I)
L	panel length
M	bending moment caused by bow in panel
M_x	applied bending moment used in figure A1
$N(\mu,\sigma)$	normal (Gaussian) distribution; μ is the mean, σ is the standard deviation
N_x	longitudinal compressive load per unit length
N_{xE}	Euler buckling load of panel
N_{xy}	shear load per unit length
N_y	transverse compressive load per unit length
n	integer; number of buckling half-waves in x-direction
P	probability
Q	lateral pressure loading on panel in figure A1
R	reliability; probability that structure can carry a specified load
t_i	ply thicknesses
X, Y, Z	Cartesian coordinate axes defined in figure 1
x, y, z	coordinate directions
ε_x	strain in x-direction
θ	ply orientation angle
λ	half-wavelength of buckling mode in x-direction
μ	mean value of a distribution
μ_{12}	Poisson's ratio of composite ply in coordinate system defined by fiber direction (table I)
σ	standard deviation of a distribution
Φ	standard cumulative distribution function

Summary of Analysis-Design Procedure

The two composite panels in this report were obtained from a computer program for analyzing and sizing uniaxially stiffened composite panels. The computer program, denoted PASCO (refs. 12–16), incorporates an eigenvalue buckling analysis, a stress analysis, and an optimization procedure. The optimization procedure adjusts the values of design variables (ply thicknesses and plate widths) to obtain the minimum-weight panel design that, for a specified design load, does not violate behavioral constraints. For this case, the constraints prevent buckling and excessive strains. All calculations in this analysis-design procedure are deterministic.

The PASCO program is also used to calculate the response of these two composite panels when they have an initial bow-type imperfection. When a panel is compressed, the bow causes a bending moment that affects the stress distribution. Depending upon whether the bow is positive or negative, the bending moment causes additional compressive stresses in the skin or in the extreme fibers of the stiffener, respectively. These additional stresses generally reduce the buckling load. A panel with a bow and with the loading considered in this report is shown in figure 1. The bow is in the shape of a half-sine wave along the length. The size of the bow at panel midlength ($x = L/2$) is denoted e. In figure 1, e is positive. Additional information on the analysis-design procedure is presented in appendix A.
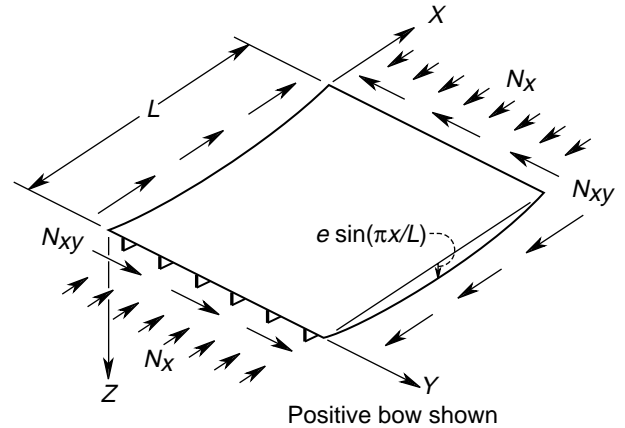

Figure 1. Stiffened panel with initial bow, applied loading, and coordinate system.

Design Studies—No Initial Bow

Two rectangular, graphite-epoxy, blade-stiffened panels were designed to carry combined compression and shear loadings. The panels were designed as if they were perfectly flat. The main difference between the two panels is the intensity of the loading; one panel is lightly loaded, the other is heavily loaded. The section that follows describes the general configuration of the two panels. The second section

describes the design requirements. The third section describes the final designs. Graphite-epoxy ply properties used in the analysis are given in table I.

Table I. Properties of Unidirectional Graphite-Epoxy Material Used in Calculations

Symbol	Value
E_1	21.0×10^6 psi
E_2	2.1×10^6 psi
G_{12}	1.0×10^6 psi
μ_{12}	0.38

General Panel Configuration

The graphite-epoxy panels contain six equally spaced stiffeners, are 30 in. long, and are simply supported on all four edges. The overall shape and loading are shown in figure 2. For each panel, the skin, blade, and attachment flange are balanced symmetric laminates made up of $\pm 45°$, $0°$, and $90°$ plies. Fiber orientation is indicated by the angle θ, which is measured with respect to the x-direction as shown in figure 2. The panels are intended to represent the design shown in figure 3, in which a representative portion of the laminated panel skin and the laminated blade with attachment flange are shown separated from one another.
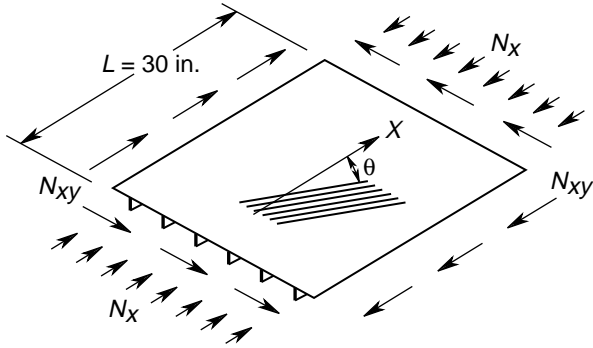

Figure 2. Overall shape and loading for two graphite-epoxy panels. Panels are designed as if flat.

The mathematical model used for analysis and design is somewhat idealized compared with the design concept shown in figure 3. The mathematical model of the skin is the same as in figure 3, but the region where the blade joins the attachment flange is different. The mathematical model, including the ply orientation angles and stacking sequence, is shown in figure 4. Seven ply thicknesses ($t_i, i = 1, 2, \ldots, 7$) and the depth b of the blade serve as design variables. Ply thicknesses are assumed to vary continuously.
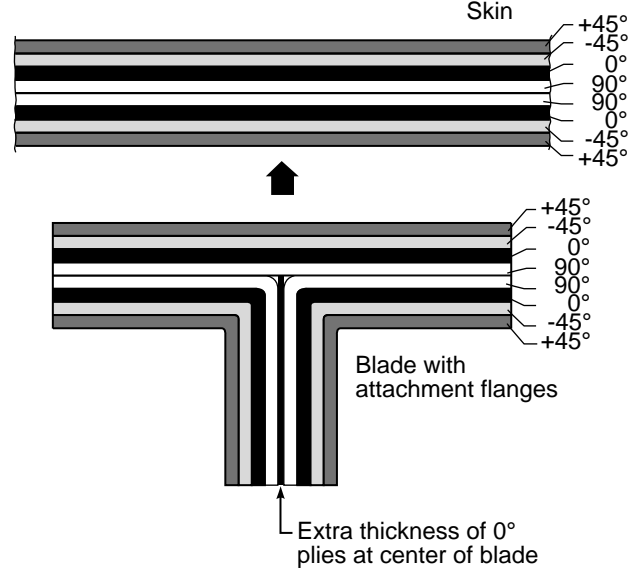

Figure 3. Design concept for skin, blade, and attachment flanges. Angles indicate ply orientation. Not to scale.
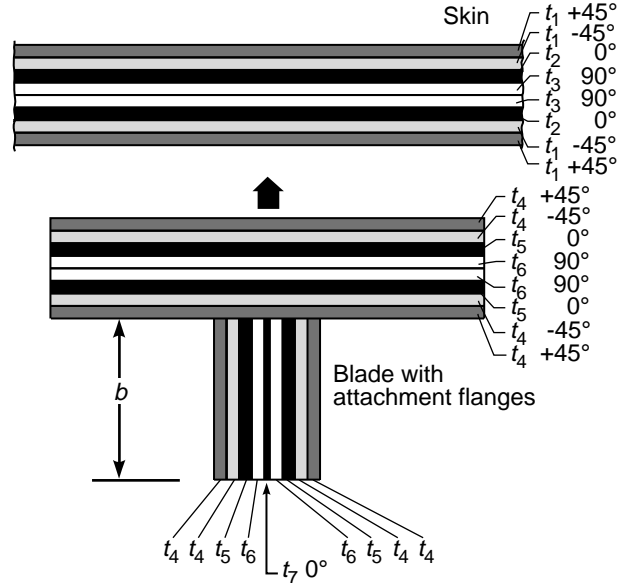

Figure 4. Mathematical model of design concept of figure 3. Used for analysis and sizing. Design variables b and t_i are shown. Angles indicate ply orientation for each t_i. Not to scale.

Design Requirements

The design requirements are the loading and the constraints. The loading is combined in-plane compression N_x and in-plane shear N_{xy}. Constraints are placed on buckling and in-plane strains at the ply level. For manufacturing and cost considerations, the attachment flange width and the stiffener spacing are fixed values. The design requirements for the two panels are as follows:

Lightly loaded panel

- Design load: $N_x = 3000$ lb/in. and $N_{xy} = 1000$ lb/in.

- Requirements on dimensions are given in figure 5.

Heavily loaded panel

- Design load: $N_x = 25\,000$ lb/in. and $N_{xy} = 5000$ lb/in.

- Requirements on dimensions are given in figure 6.

Both panels

- Panels carry their design load without buckling.

- Panels carry design load without exceeding ply-level, in-plane strains of ± 0.005 in both the fiber direction and transverse to fiber direction, and ± 0.01 shear strain—in any ply.
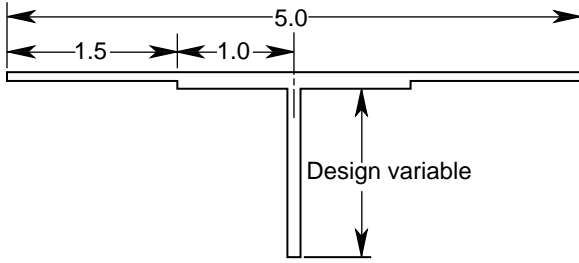

Figure 5. Design requirements on dimensions of cross section for lightly loaded panel. One repeating element is shown. Dimensions are in inches.
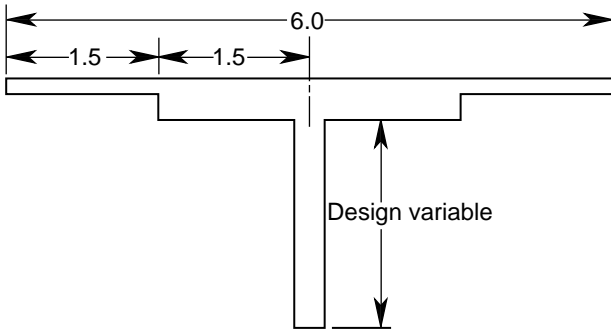

Figure 6. Design requirements on dimensions of cross section for heavily loaded panel. One repeating element is shown. Dimensions are in inches.

Final Designs

The designs obtained using PASCO are defined in figures 7 and 8 and table II. Dimensions within figures 7 and 8 are to scale. Only a repeating element is shown. As stated earlier, the panels consist of six equally spaced stiffeners and are 30 in. long. Because of the design requirements on stiffener spacing, the lightly loaded panel is 30 in. wide; the heavily loaded panel is 36 in. wide.

Table II. Design Variables (Ply Thicknesses t_i and Blade Depth b) for Two Minimum-Weight Designs

Design variable	Ply angle θ for t_i, deg	Value of design variables, in.	
		Lightly loaded design	Heavily loaded design
t_1	± 45	0.018899	0.026711
t_2	0	.002566	.012936
t_3	90	.001104	.001425
t_4	± 45	.006315	.013404
t_5	0	.019658	.096217
t_6	90	[a].001000	[a].001000
t_7	0	.038390	.066144
b		1.448772	2.035960

[a]Lower bound.

For both panels the skin consists mainly of $\pm 45^\circ$ plies with a small amount of 0° and 90° material in the center. Also, the attachment flange and blade consist mainly of 0° plies. The thicknesses of the plies at each angle are indicated in figures 7 and 8 by the various layers in each plate element. To account for bending moments produced by the bow, the blade is modeled in four segments, each $b/4$ deep, and each capable of carrying a different axial load. (See figs. 7 and 8.) The bending moment is accounted for (approximately) by the variation in the axial load among the four segments, the attachment flange, and the skin (ref. 11). The larger the number of segments, the better the approximation.

Both panels buckle at the design load; for each panel, two buckling modes are critical. One of these two modes has a longitudinal half-wavelength λ that is equal to the panel length L. The other mode has a longitudinal half-wavelength that is shorter than the panel length. For the lightly loaded panel, the two buckling modes are shown in figures 9(a) and 9(b). Both figures are contour plots of the lateral deflection of the skin. The $\lambda = L$ mode shown in figure 9(a) is from the adjusted analysis technique[1] mentioned

---

[1]When calculating the buckling load of a finite rectangular stiffened plate that is loaded by in-plane shear (N_{xy}), the analyst can generally assume that correct boundary conditions at the ends of the panel ($x = 0$, $x = L$) are more important than correct boundary conditions along the sides that are parallel to
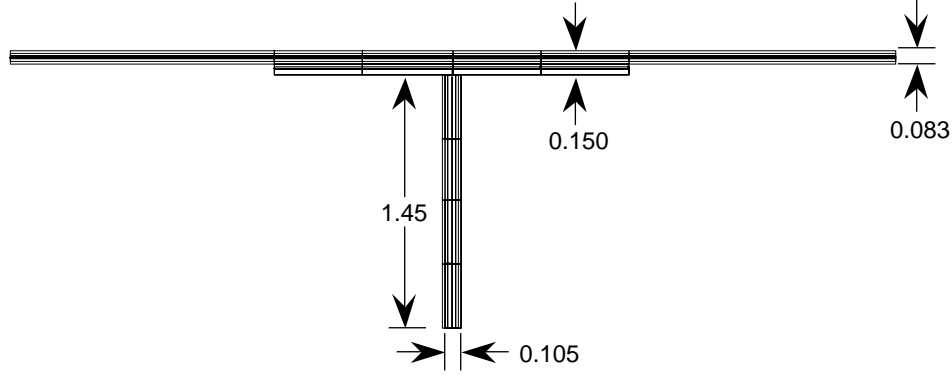
Figure 7. Final design for lightly loaded panel. One repeating element is shown. Dimensions are in inches.
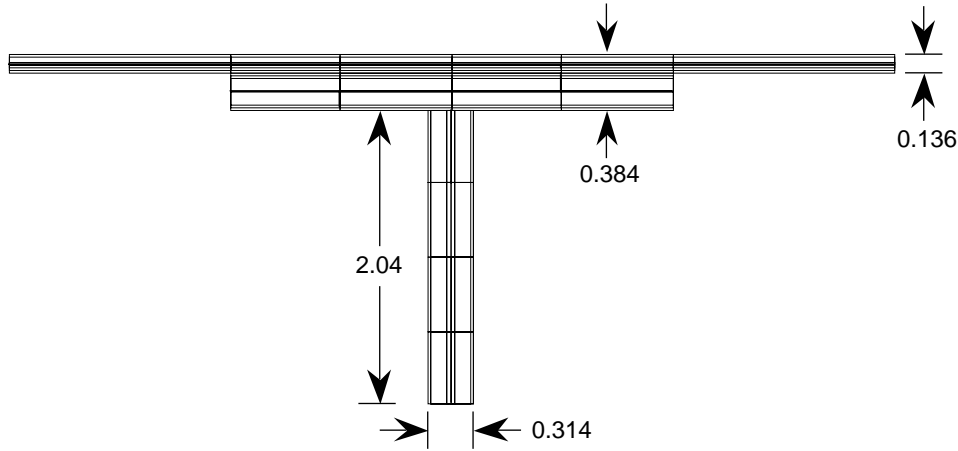

Figure 8. Final design for heavily loaded panel. One repeating element is shown. Dimensions are in inches.

in appendix A and described in references 12, 13, and 16. The mode shape shown in figure 9(b) has a longitudinal half-wavelength of $\lambda = L/5$. Although the buckling mode shape in figure 9(b) does not satisfy simple support boundary conditions at the ends of the panel, the buckling wavelength is short enough for the mode to develop in the center portion of the panel. For the heavily loaded panel, the two buckling modes are for $\lambda = L$ and $\lambda = L/2$. In addition to being buckling critical at the design load, the heavily loaded panel is also strain critical at the design load.

The contour plots shown in figure 9 were obtained with the computer program VICONOPT (refs. 20–23) which, in many ways, is the successor to the PASCO program.

Effect of Initial Bow on Failure Load

Both minimum-weight panels described in the previous section were analyzed under the assumption that they had various amounts of initial bow. The bow is in the form of a half-sine wave along the length. The failure load of the panel is assumed to be the lower of the buckling load and the load at which any strain exceeds the corresponding ply-level allowable strain given in the section "Design Requirements." The results for the lightly loaded panel are shown in figure 10; the results for the heavily loaded panel are shown in figure 11. In both figures, the ratio of the failure load to the design load is shown as a function of e, the size of the bow (fig. 1). Note that the curves are not symmetric with respect to the line $e = 0$.

---

the stiffeners. This assessment is particularly true if the buckling half-wavelength λ in the x-direction is equal to the panel length L. In a discrete stiffener solution, VIPASA (refs. 17–19), which is the buckling analysis within PASCO, can account for boundary conditions along the sides of the panel, but the VIPASA program cannot account for boundary conditions along the ends. However, with a smeared stiffener solution, the panel can be rotated 90° and boundary conditions can be placed on the ends of the panel. That smeared stiffener solution, which is denoted $F_{s,90}$ in reference 13, is shown in figure 9(a).

Figure 10. Variation of nondimensional failure load with initial bow for lightly loaded panel. For this case, the failure mode is buckling.

(a) Mode for which $\lambda = L$; Buckling load/Design load = 0.99798.
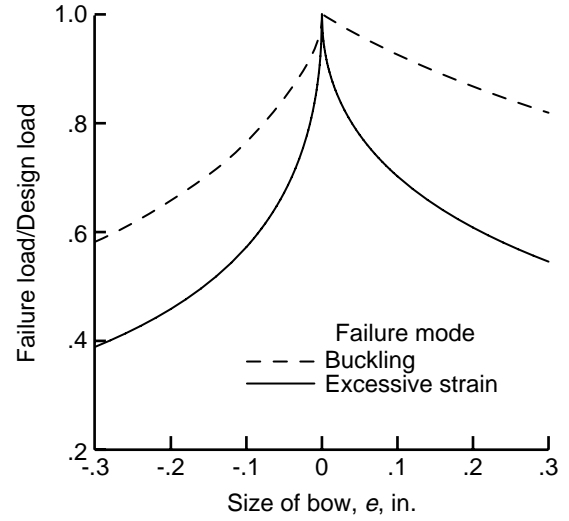
Figure 11. Variation of nondimensional failure load with initial bow for heavily loaded panel.

(b) Mode for which $\lambda = L/5$; Buckling load/Design load = 1.00265.

Figure 9. Buckling mode shapes for flat, lightly loaded panel under design loading of $N_x = 3000$ lb/in. and $N_{xy} = 1000$ lb/in.

When the panel is compressed, the bow produces large bending strains that are added to the uniform axial strains of the flat panel. A positive value of e adds compression to the skin; a negative value of e adds compression to the tip of the blade. For the lightly loaded panel (fig. 10), the failure mode is buckling. For example, at $e = -0.1$ in., the panel buckles at about 0.57 times the design load. Both components of the design load vector are multiplied

by the same factor to obtain the failure load vector, as shown in equation (1):

$$\begin{bmatrix} N_x \\ N_{xy} \end{bmatrix}_{\text{failure}} \approx 0.57 \begin{bmatrix} N_x \\ N_{xy} \end{bmatrix}_{\text{design}} = 0.57 \begin{bmatrix} 3000 \\ 1000 \end{bmatrix} = \begin{bmatrix} 1710 \\ 570 \end{bmatrix} \quad (1)$$

For this example of $e = -0.1$ in., the buckling mode has a longitudinal half-wavelength of $\lambda = L/9$.

For the heavily loaded panel (fig. 11), the failure mode is excessive strain (material strength failure). For reference, the curve for buckling is also shown in figure 11. At $e = 0$, buckling and excessive strain occur simultaneously at the design load. For other values of e, excessive strain occurs at a lower load than the buckling load.

Additional information on the analysis of a panel with a bow is given in appendix A. For both panels, the variation of the failure load with e is tabulated in appendix B so that reliabilities can be calculated for distributions of the bow not considered herein.

Reliability

A structure's reliability is defined as the probability that it will perform its intended function without failing. In the present context, the reliability is the probability that the panel will carry a given load without buckling or exceeding allowable strains. In general, to calculate the reliability, two types of information are needed: first, the relationship between the failure load of the panel and the values of the random variables; second, the joint probability density of the random variables.

In this report, a single random variable is considered—the size e of the bow. The first type of information, the failure load as a function of e, is obtained with PASCO and is illustrated in figures 10 and 11. In subsequent sections of this report, the size e of the bow is assumed to have various, specified probability densities.[2] This assumption provides the second type of information.

---

[2]In this report, each distribution is assumed. Quantitative procedures to help determine the validity of an assumed distribution are *goodness-of-fit* tests. Two examples are the chi-square and Kolmogorov-Smirnov tests. In both tests, comparisons are made between the observed experimental data and the corresponding data from the assumed theoretical distribution. If differences between the two sets of data are sufficiently small, the assumed distribution is accepted. Hypothesis test procedures are used to determine a "sufficiently small difference." In such procedures, an acceptable difference is defined based on the number of samples in the experimental data and on the significance level that is adopted. In the final analysis, engineering judgment as

In the first section below, e is assumed to have a normal distribution; the reliability of the two panels is examined for three values of the standard deviation. In the second section, the distributions considered for e are a normal distribution and two extreme value distributions, all with the same mean and same standard deviation. In the third section, the distributions are similar to those in the second section, except that the distributions are truncated; a value of e larger than a specified value is not allowed. Studies are presented that show the effect of these distributions on the reliability of the two panels. Sample calculations that illustrate reliability concepts are given in appendix C.

Bow With Normal Distribution

In this section, the value of e is assumed to have a normal distribution $N(\mu, \sigma)$, where μ is the mean and σ is the standard deviation. For this report, the mean value of e is taken to be zero; that is, $\mu = 0$. In this section, three values of the standard deviation are considered: $\sigma = 0.01, 0.02$, and 0.05 in. The probability density functions for these three distributions of e are shown in figure 12.
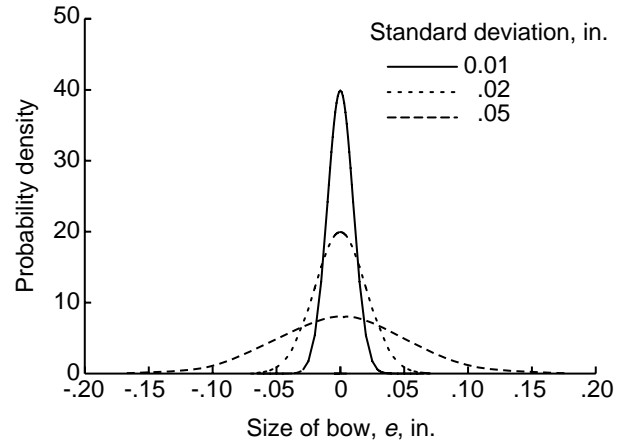
Figure 12. Probability densities for three normal distributions of bow.

The reliability of the lightly loaded imperfect panel at various load levels is presented in figure 13. The reliability of the heavily loaded imperfect panel is presented in figure 14. (For reference, the reliability of a perfectly flat panel is also shown in figs. 13 and 14.) At low load levels (Applied load/ Design load ≤ 0.4), the reliability is approximately unity for both imperfect panels, regardless of the

---

well as quantitative measures of goodness of fit are used to define the distribution (refs. 24–27).
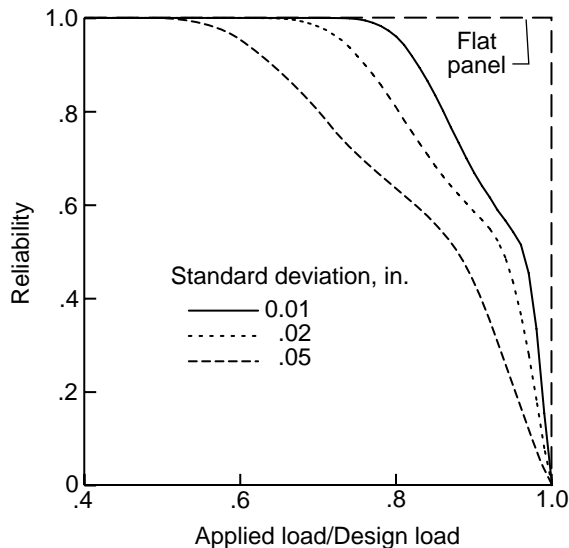
Figure 13. Reliability of lightly loaded panel versus ratio of applied load to design load for three distributions of initial bow. The probability densities for these three distributions are given in figure 12. Reliability of perfectly flat panel is also shown.
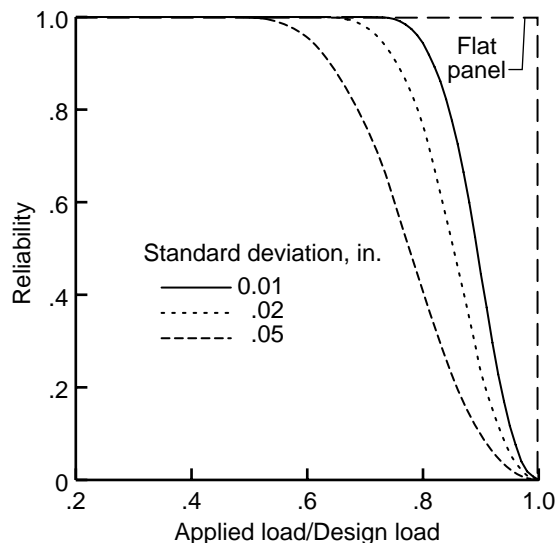
Figure 14. Reliability of heavily loaded panel versus ratio of applied load to design load for three distributions of initial bow. Probability densities are given in figure 12. Reliability of perfectly flat panel is also shown.

distribution of the bow. For higher load levels, the reliability decreases and depends strongly upon the distribution of the bow. When the applied load is equal to the design load, the reliability is zero.

The reliability curves in figures 13 and 14 illustrate the importance of accounting for a bow. Even

with a bow standard deviation of only 0.01 in., the reliability is substantially reduced compared with a perfectly flat panel. These results also indicate the sensitivity of the reliability to the statistical parameters, such as the standard deviation.

The curves can be interpreted in the following way. Assume that the goal is to have a reliability of 0.99 after accounting for the bow. Assume, also, that the design process ignores the bow but uses a knockdown factor to account for uncertainty. For the heavily loaded panel with a bow standard deviation of 0.05 in., the reliability is 0.99 at Applied load/Design load ≈ 0.55. Thus, the required knockdown factor k would be 0.55. Equivalently, the bow can be ignored but the design load increased by 82 percent $(1/k = 1.82)$. If, for example, a 50-percent higher load is used, the reliability is only 0.85 $(R = 0.85$ at Applied load/Design load $= 0.66)$. Similar results occur for the lightly loaded panel.

Bow With Normal and Extreme Value Distributions

In this section, a comparison is made between the reliabilities of panels with three different distributions of the bow: a normal distribution, a type I asymptotic distribution of maximum extreme values (maximum extreme value distribution), and a type I asymptotic distribution of minimum extreme values (minimum extreme value distribution).[3] Parameters that define the three distributions are selected so that all three distributions have the same mean and same standard deviation $(\mu = 0$ in. and $\sigma = 0.02$ in.). Only the higher statistical moments differ. The probability density functions for the three distributions are shown in figure 15. The statistical parameters for these distributions are given in appendix D along with the distribution functions.

Results for the lightly loaded panel are presented in figure 16 and for the heavily loaded panel in figure 17. In each case only the high-reliability

---

[3]Extreme value distributions are important for engineering applications These distributions can be used to describe the maximum or minimum values from random phenomena such as wind speed, wave heights, and rainfall. The phenomena have distributions, but only the maximum or minimum values of the phenomena are of interest, not the average or typical values. If a phenomenon has a distribution with an exponentially decaying tail in the direction of interest (to the right is maximum, etc.), the corresponding extreme value distribution is denoted type I. A normal distribution is an example of a distribution with exponentially decaying tails in both directions. For information on extreme value distributions, see references 26 and 28.
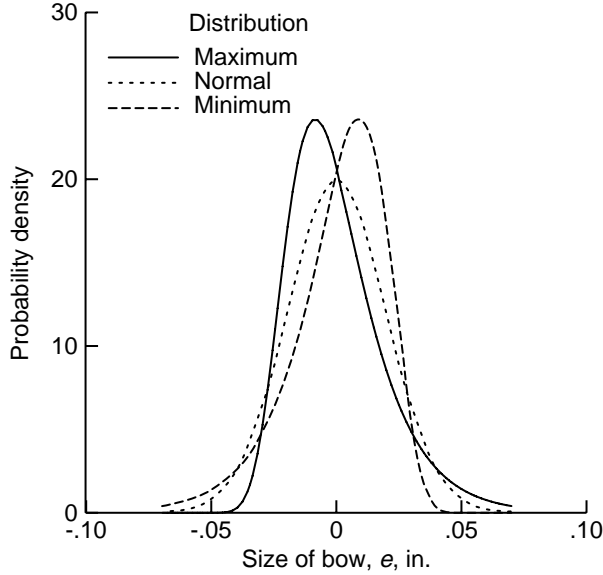
Figure 15. Probability densities for three distributions of bow: maximum extreme value, normal, and minimum extreme value. Each distribution has a mean of zero and a standard deviation of 0.02 in.

Figure 16. Reliability of lightly loaded panel versus ratio of applied load to design load for three distributions of bow. Probability densities are given in figure 15.

Figure 17. Reliability of heavily loaded panel versus ratio of applied load to design load for three distributions of bow. Probability densities are given in figure 15.

portions of the curves are shown. Even though the means and standard deviations of the imperfections are equal, the curves in each figure are different. These differences demonstrate that the reliability of an imperfect panel depends upon the details of the probability density of the imperfection. The results can be interpreted in the following two ways.

First, suppose that three panel fabrication processes produce the same mean and standard deviation for an imperfection. The results indicate that, with these limited data, we cannot assume that the three fabrication processes are equivalent. The distributions could differ; therefore, one of the processes could be considerably better because it could produce panels with a higher reliability than the other two.

Second, suppose only one fabrication process exists and only the first two moments of the imperfection (the mean and the standard deviation) are known. To calculate the performance of the panels, the analyst must assume the distribution of the imperfection; therefore, the higher moments are assumed. The results indicate that the calculations will be sensitive to the assumptions. The common assumption of a normal distribution can be conservative or unconservative.

Bow With Truncated Normal and Truncated Extreme Value Distributions

In practice, quality control procedures would eliminate panels with a bow larger than a specified

maximum value. For that reason, the large tails on the probability density functions (e.g., fig. 15) are unrealistic. Using truncated distributions is one way to study panel reliability and account for such quality control measures.

In this section, the distributions of the bow are similar to those of the previous section, except that

9

the distributions are truncated. For these studies, the absolute value of the maximum bow (e_{max}) is selected to be 0.04 in. Because the standard deviations of the original untruncated distributions are 0.02 in., the maximum bow is $\pm 2\sigma$ of the original, untruncated distributions. The probability density functions for these distributions are shown in figure 18.

Figure 18. Probability densities for three truncated distributions. Original probability densities are given in figure 15. Truncations occur at $e = \pm 0.04$ in.

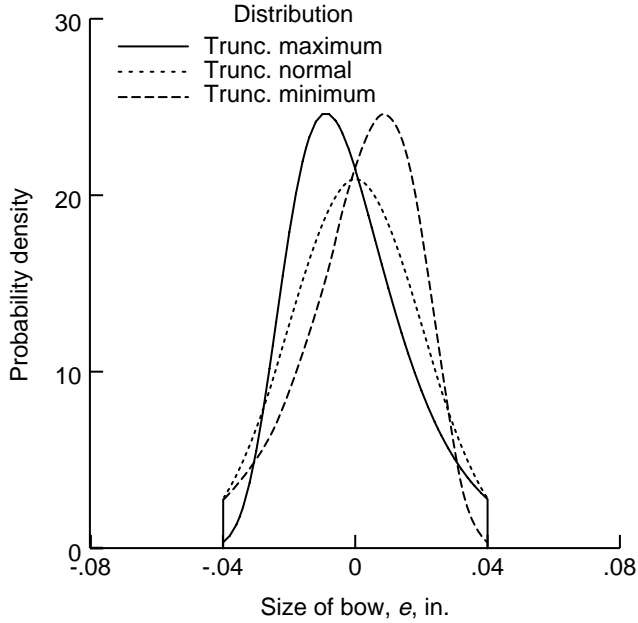The reliability of panels with these distributions of e is shown in figures 19 and 20. (The lightly loaded panel is in fig. 19 and the heavily loaded panel is in fig. 20.) For comparison, the figures also include the reliabilities of the panel if the distributions are not truncated.

The results indicate that if the original distribution is minimum extreme value, an e_{max} of $\pm 2\sigma$ provides panels that are substantially more reliable. If the distribution is normal, an e_{max} of $\pm 2\sigma$ provides panels that are moderately more reliable. If the distribution is maximum extreme value, an e_{max} of $\pm 2\sigma$ has negligible effect on panel reliability. The results also indicate that even with truncated distributions, the reliability is sensitive to details of a distribution, but less sensitive for the truncated distribution than for the untruncated one.

Concluding Remarks

Analytical studies were conducted on two minimum-weight, stiffened panels—designed as if
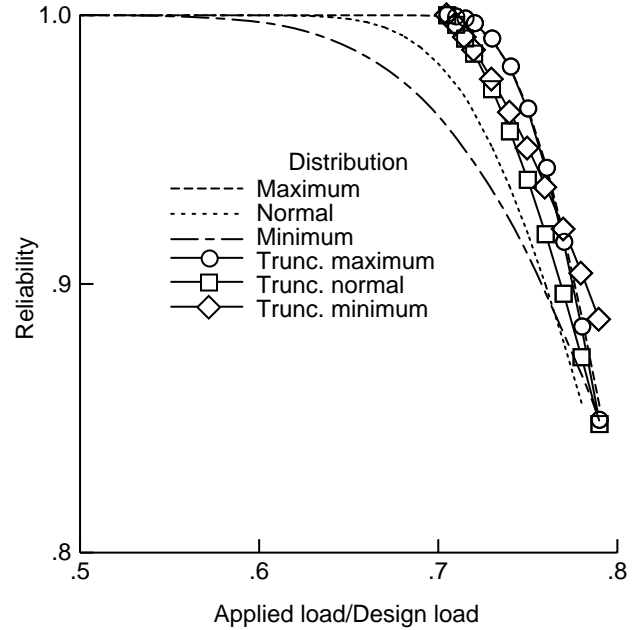
Figure 19. Reliability of lightly loaded panel for original and truncated distributions of figures 15 and 18, respectively.
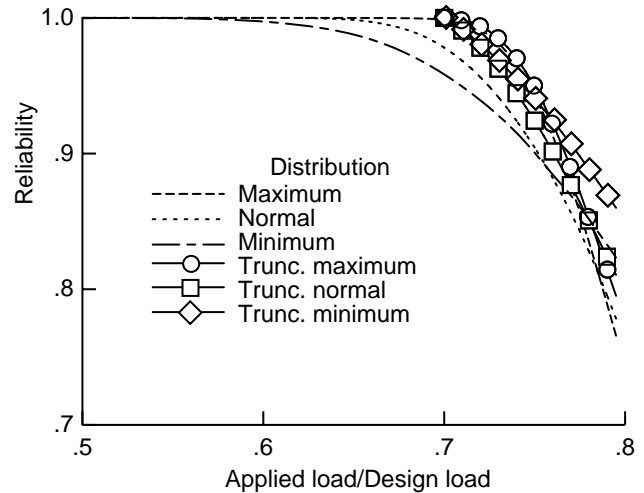
Figure 20. Reliability of heavily loaded panel for original and truncated distributions of figures 15 and 18, respectively.

they were flat—to determine the extent to which a small overall bow could degrade their reliability. The loading case was combined compression and shear. The degradation in reliability was found to be substantial. This report also demonstrates the importance of accurate specification of bow statistics and illustrates an approach used to make reliability calculations.

Just as a bow-type imperfection increases the bending stresses and reduces the buckling load of a

panel, it also reduces the reliability of a panel. In one case, if the bow has a normal distribution with a mean of zero and a standard deviation of 0.05 in., a panel designed as if it were flat would require a design safety factor of about 1.8 to achieve a reliability of 0.99. Accounting for additional uncertainties would require a larger safety factor.

To determine the sensitivity of the reliability to details of the bow statistics, studies were made with three distributions of the bow. All distributions had the same mean and same standard deviation. Only the higher statistical moments differed. The three distributions were normal, maximum extreme value, and minimum extreme value. Although the probability density functions had the same general shape, the panel reliabilities were quite different. These differences indicate that the reliability is sensitive to the details of the bow distribution. This sensitivity should be taken into account when engineers make assumptions regarding the probability density of the bow and select a fabrication process.

Good quality control would eliminate panels with a bow larger than a specified maximum value. To examine the effect of quality control, panel reliability was studied for bows with truncated distributions. The basic distributions were the same three types mentioned above. The maximum value of the bow was set at ± 0.04 in., which, for the example selected, is twice the standard deviation of the untruncated distributions. For two distributions (minimum extreme value and normal), truncating the distributions caused the reliability to improve; for the remaining distribution (maximum extreme value), the

reliability was unchanged. The reliability is less sensitive to the statistical details of the imperfection when the distributions are truncated.

Several reliability computations are illustrated in appendix C. With a single random variable, as is the case in this report, the probabilistic computations are straightforward. They are included for illustrative purposes.

The studies emphasize the need for engineers to account for imperfections when they design structural members. Probabilistic methods can help account for imperfections when these imperfections contain uncertainties. One approach is to consider the imperfections as random quantities with statistical distributions. The structure could be designed to minimize the weight or cost and still meet a specified reliability, or the structure could be designed to maximize the reliability for a given cost or weight. Because an increase in quality control could provide a decrease in imperfections, which in turn, could allow a decrease in structural weight, cost comparisons could include quality control and structural weight. For example, cost trade-offs could be performed between two equally reliable structural designs: a lightweight design that requires considerable quality control and a heavier design requiring less quality control.

Appendix A

Analysis and Design Procedures

Buckling Analysis

The buckling analysis used to obtain the results presented in this report is contained in the PASCO computer program, which analyzes and sizes uniaxially stiffened (prismatic) composite panels subject to the loading shown in figure A1. The PASCO program (refs. 12–16) incorporates an earlier computer program, VIPASA (refs. 17–19).
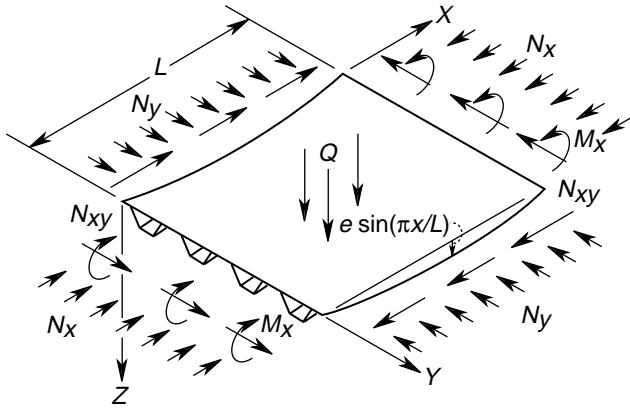

Figure A1. Stiffened panel with initial bow, applied loading, and coordinate system. Figure indicates analysis capabilities of PASCO.

The analysis treats an arbitrary assemblage of plates, each with a combined in-plane loading of N_x, N_y, and N_{xy}. The response of each plate element making up the stiffened panel is obtained from an exact solution to the thin-plate equations. The analysis connects these individual plate elements and maintains continuity of the buckle pattern across the intersection of neighboring plate elements. All quantities that define the analysis problem (the panel cross section, loading, boundary conditions, etc.) are assumed to be uniform in the x-direction (fig. A1). The buckle patterns in the x-direction are taken to be sine waves whose half-wavelengths λ are fractions $(1/n)$ of the panel length (e.g., $\lambda = L$, $L/3$, $L/9$, etc.). For orthotropic panels loaded only by N_x and N_y, the solution is exact for panels that are simply supported along the edges $x = 0$ and $x = L$.

The VIPASA program underestimates the buckling load when the loading involves shear and the buckling mode is skewed, with a longitudinal buckle length equal to the length of the panel ($\lambda = L$). The PASCO program contains an approximate approach, the adjusted analysis technique, to overcome that

limitation. The basis for the limitation in VIPASA and the adjusted analysis technique in PASCO are described in reference 16. Because the loadings considered in the present report involve shear, the adjusted analysis technique is used.

Analysis for Initial Bow-Type Imperfection

The VIPASA analysis (hence, the PASCO analysis) cannot treat panels that are curved in the x-direction. The approach used in PASCO is to treat the panel as flat (which allows boundary conditions to be imposed on the sides), but to use a stress distribution for a panel with a bow. The bow is in the shape of a half-sine wave down the length. The following description of the analysis technique is taken verbatim from reference 11:

> The approach used here to account for the effect of an initial bow in the panel is the same as that used in reference 2 [10] (with appropriate changes to account for laminated walls). The panel is assumed to have the initial bow shown in figure 1 [A2]. The stresses acting on the panel cross section are taken to be the sum of the stress from N_x and the stress resulting from the moment caused by the bow. In terms of the longitudinal strain ε_x, this gives

$$\varepsilon_x = \frac{N_x}{ET} + \frac{M \cdot c}{D_x} \qquad (1[A1])$$

> The moment varies over the length of the panel. At the midlength of the panel the moment is largest and is given by

$$M = \frac{N_x \cdot e}{1 - \frac{N_x}{N_{xE}}} \qquad (2[A2])$$

> in which N_{xE} is the Euler or wide-column buckling load of the panel. The denominator in equation (2[A2]) gives the nonlinear effect of the deformation growing with the applied load. Except for one wavelength, the buckling calculations are made assuming that the midlength stresses from equations (1[A1]) and (2[A2]) are the stresses over the entire length of the panel. The exception is the buckling mode having a half-wavelength λ equal to the panel length L. For that case, the moment M is considered to be zero. The initial bow in the panel does not, therefore, directly affect the $\lambda = L$ buckling load.
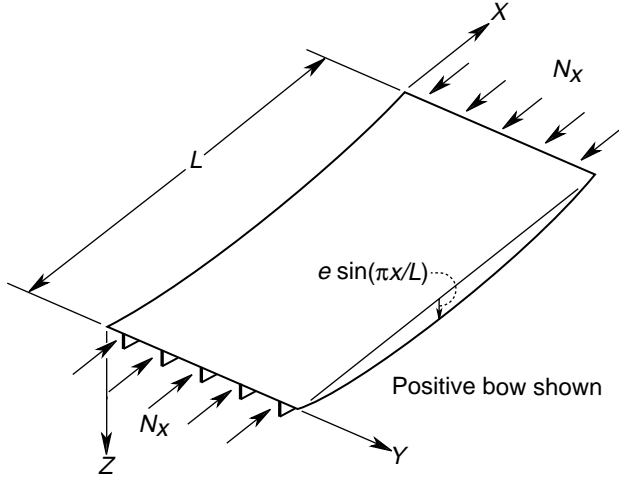
Figure A2. Panel with initial bow.

As pointed out in reference 13, strictly speaking, equations (1[A1]) and (2[A2]) are appropriate only when N_x is the sole in-plane load. However, in PASCO these equations are applied to problems with combined loads. For the combined load cases of N_x *and* N_{xy} considered in the present report, equation (2[A2]) is rewritten as

$$M = \frac{N_x e}{1 - \gamma} \qquad (A3)$$

where the parameter γ is defined as

$$\gamma = \frac{F}{F|_{\lambda = L}} \qquad (A4)$$

in which F is a scalar defined by

$$F \begin{bmatrix} N_x \\ N_{xy} \end{bmatrix}_{\text{design}} = \begin{bmatrix} N_x \\ N_{xy} \end{bmatrix}_{\text{failure}} \qquad (A5)$$

The design load vector on the left in equation (A5) is scaled up or down with the parameter F to obtain that combination that causes buckling or strains that exceed allowables. The quantity $F|_{\lambda = L}$ is the value of F for the lowest buckling load for which the buckling half-wavelength λ is equal to the panel length L. In figures 10 and 11, the ratio of failure load to design load is the same as the parameter F.

The above approach for treating a bow is an approximate one that captures the main features of the physical problem. Because it is computationally efficient, the approach can be used for optimization. It is also reasonably accurate, as is seen in reference 12, where Anderson and Stroud compare analysis with test results.

Sizing

The computerized structural sizing approach used in PASCO is based on nonlinear mathematical programming techniques. The computer program CONMIN (refs. 29 and 30) is the optimizer within PASCO. Sizing variables are automatically adjusted to obtain the design that minimizes an objective function subject to a set of inequality constraints. Taylor series expansions of the constraints are used to improve computational efficiency.

For the studies presented in this report, the sizing variables are widths of plate elements and thicknesses of composite plies that make up the plate elements; the objective function is the panel weight. Inequality constraints are placed on buckling loads and in-plane strains in each ply. The strain constraints are placed on in-plane shear strains and on strains that are tangential and normal to the fiber direction—in each ply.

Appendix B

Failure Load as a Function of Size of Initial Bow

For the two panels discussed in the section "Final Designs," the failure load as a function of the size of the initial bow is given in tables BI and BII. Numerical values are provided so that reliabilities can be calculated for distributions of the bow not considered herein.

For the lightly loaded panel, table BI gives the ratio of failure load to design load (F in eq. (A5)) as a function of size e of bow. Failure for this panel is buckling. These data are used to produce the curve in figure 10.

Comparable data for the heavily loaded panel are given in table BII. Failure for this panel is excessive strain (material strength) in the prebuckling stress state. These data are used to produce the lower curve in figure 11.

Table BI. Ratio of Failure Load to Design Load as Function of Size of Bow for Lightly Loaded Panel

[For this panel, failure is buckling]

Bow, e, in.	Failure load / Design load	
	Negative bow	Positive bow
0.000	0.9980	0.9980
.001	.9552	.9959
.002	.9348	.9938
.003	.9190	.9919
.004	.9054	.9898
.005	.8934	.9878
.006	.8827	.9859
.007	.8729	.9839
.008	.8639	.9820
.009	.8555	.9803
.010	.8476	.9783
.012	.8331	.9747
.014	.8199	.9713
.016	.8078	.9678
.018	.7966	.9642
.020	.7861	.9609
.025	.7625	.9528
.030	.7417	.9450
.035	.7231	.9375
.040	.7062	.9303
.045	.6906	.9234
.050	.6763	.9166
.055	.6627	.9101
.060	.6500	.9038
.065	.6381	.8977
.070	.6269	.8917
.075	.6163	.8859
.080	.6062	.8802
.085	.5966	.8747
.090	.5874	.8693
.095	.5786	.8641
.100	.5702	.8589
.120	.5398	.8395
.140	.5134	.8215
.160	.4901	.8047
.180	.4694	.7890
.200	.4508	.7741
.220	.4338	.7600
.240	.4183	.7465
.260	.4041	.7337
.280	.3910	.7216
.300	.3788	.7099

Table BII. Ratio of Failure Load to Design Load as Function of Size of Bow for Heavily Loaded Panel

[For this panel, failure is excessive strain]

Bow, e, in.	Failure load / Design load	
	Negative bow	Positive bow
0.000	1.001	1.001
.001	.9453	.9654
.002	.9234	.9513
.003	.9070	.9406
.004	.8934	.9317
.005	.8816	.9239
.006	.8710	.9170
.007	.8614	.9103
.008	.8526	.9043
.009	.8444	.8992
.010	.8367	.8940
.012	.8226	.8845
.014	.8099	.8759
.016	.7982	.8679
.018	.7874	.8604
.020	.7773	.8535
.025	.7546	.8377
.030	.7348	.8236
.035	.7170	.8110
.040	.7008	.7993
.045	.6861	.7886
.050	.6723	.7786
.055	.6596	.7691
.060	.6477	.7603
.065	.6365	.7519
.070	.6259	.7438
.075	.6159	.7362
.080	.6064	.7289
.085	.5973	.7219
.090	.5886	.7152
.095	.5803	.7087
.100	.5724	.7024
.120	.5435	.6794
.140	.5185	.6589
.160	.4963	.6405
.180	.4765	.6237
.200	.4586	.6083
.220	.4424	.5940
.240	.4275	.5807
.260	.4137	.5683
.280	.4010	.5566
.300	.3892	.5456

Appendix C

Reliability and Sample Calculations

The approach used to calculate the reliability is based on the definition of the probability density function. The only random variable is the size e of the initial bow. For these sample calculations, the value of e is assumed to have a normal distribution $N(\mu, \sigma)$, where μ is the mean and σ is the standard deviation. For all studies in this report, $\mu = 0$; for these sample calculations, $\sigma = 0.05$ in. The probability density function for this distribution of e is shown in figure C1.
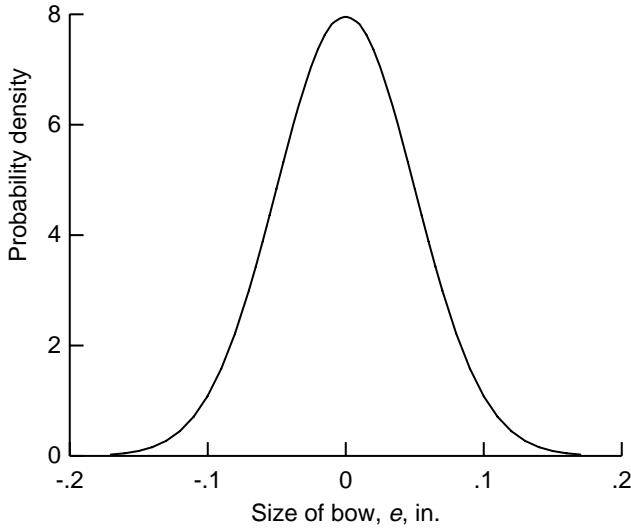

Figure C1. Probability density for normal distribution of initial bow. $\mu = 0$; $\sigma = 0.05$.

The reliability of the panel at a specified applied load is the probability that the panel failure load is equal to or greater than that specified load. In a case involving a single applied load, such as N_x, this definition of reliability is clear. However, in a case involving combined loads, such as N_x *and* N_{xy}, the term *failure load* can be ambiguous; various combinations of applied load can cause failure. In this report, all combinations of applied load are obtained by scaling the design load vector. The scale factor F (eq. (A5)) is the single parameter that defines the intensity of the applied load that causes failure. Based on that fact, the definition of panel reliability given above can be restated in terms of F as follows: the reliability R at a specified load F_s is the probability P that the panel's failure load F is

equal to or greater than that specified load F_s. This definition of reliability can be expressed as

$$R(F_s) = P(F \geq F_s) \qquad \text{(C1)}$$

Because the relationship between e and F is known or can be computed (figs. 10 and 11 and tables BI and BII), the probability that the failure load is equal to or greater than a specified load can be converted to the probability that the random variable e takes on a value within a certain range of values. That is,

$$P(F \geq F_s) = P(e_1 \leq e \leq e_2) \qquad \text{(C2)}$$

Furthermore, because e has a specified distribution—in this case a normal distribution—the right side of equation (C2) can be evaluated in a straightforward manner.

A graphical interpretation of the evaluation method is illustrated in figures C2(a) and C2(b) (adapted from fig. 5.19 in ref. 24). The failure curve for the lightly loaded panel is shown in figure C2(a); the distribution of e for $\sigma = 0.05$ in. is shown in figure C2(b). The values of e for the upper figure are aligned with those of the lower figure. Based on the definition of the probability density function, the reliability of the panel at $F = 0.80$ (for example) is equal to the shaded area in figure C2(b).

The dashed line at $F = 0.80$ intersects the failure curve at $e_1 = -0.01739$ in. and $e_2 = 0.1660$ in. (These two values of e and the four values given in eq. (C8) were obtained by a linear interpolation between data points given in table BI, not from graphs.) The area of the shaded region can be calculated by first transforming e_1 and e_2 to standardized variables $\overline{e}_1$ and $\overline{e}_2$ associated with a standard normal distribution $N(0,1)$ so that

$$\overline{e}_1 = \frac{e_1 - \mu}{\sigma} = \frac{-0.01739 - 0}{0.05} = -0.3478 \qquad \text{(C3)}$$

$$\overline{e}_2 = \frac{e_2 - \mu}{\sigma} = \frac{0.1660 - 0}{0.05} = 3.320 \qquad \text{(C4)}$$

Letting Φ denote the standard cumulative distribution function, the area A of the shaded region is given by

$$A = \Phi(\overline{e}_2) - \Phi(\overline{e}_1) \qquad \text{(C5)}$$

The function Φ can be evaluated from a table for a standard normal distribution function (see, for example, section 3.2.1 of ref. 25) or with a calculator that
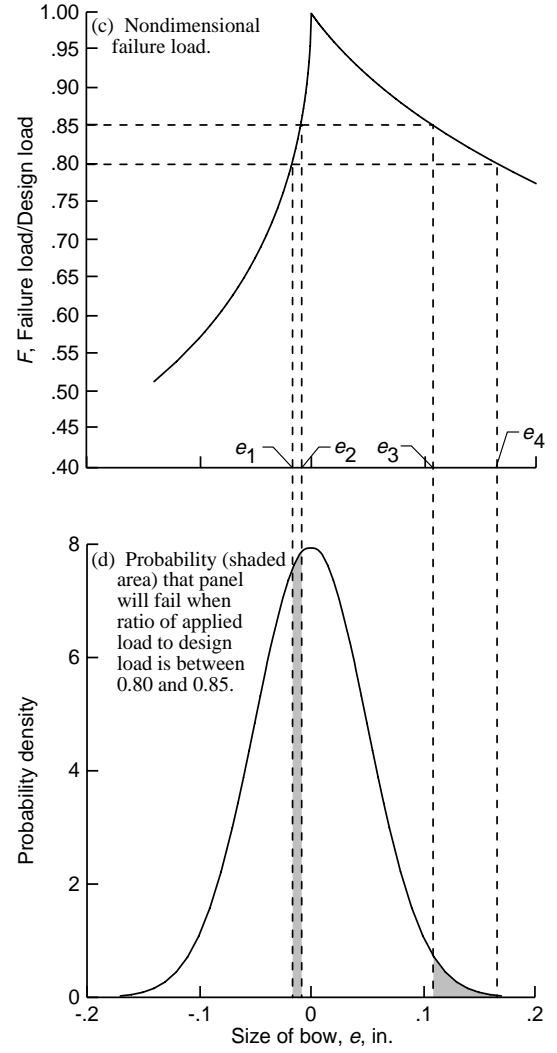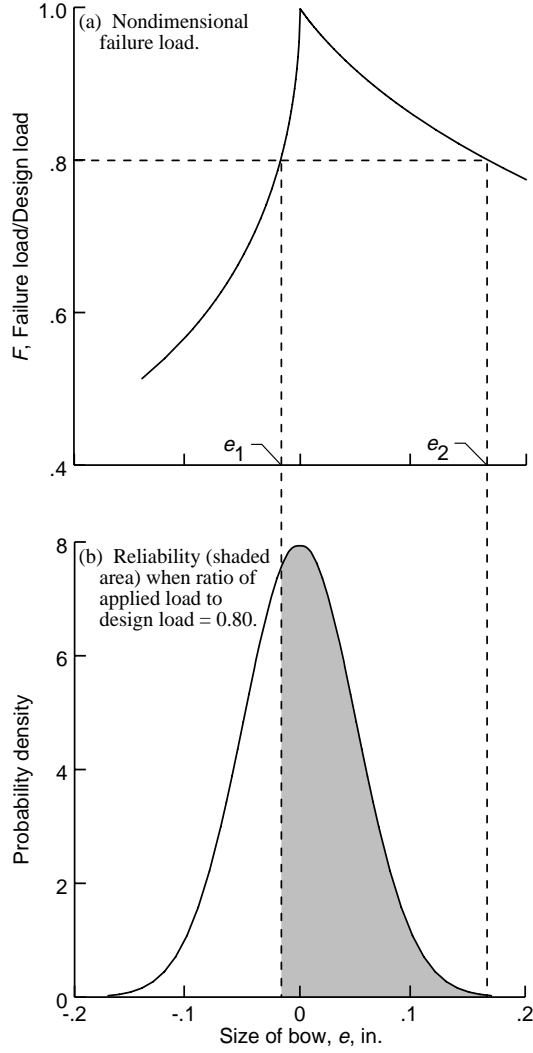
Figure C2. Graphical interpretation of procedure for calculating reliability at a specific load (figs. C2(a) and (b)) and probability of failure between two specific loads (figs. C2(c) and (d)) for lightly loaded panel with a bow probability density of $N(0.0, 0.05)$.

has a statistical mode. For this example, calculations give

$$P(e_1 \leq e \leq e_2) = A = \Phi(\bar{e}_2) - \Phi(\bar{e}_1)$$
$$= \Phi(3.320) - \Phi(-0.3478)$$
$$= 0.99955 - 0.36400$$
$$\approx 0.64 \qquad (C6)$$

Therefore, the reliability of this panel at a loading of

$$\begin{bmatrix} N_x \\ N_{xy} \end{bmatrix}_{\text{applied}} = F_s \begin{bmatrix} N_x \\ N_{xy} \end{bmatrix}_{\text{design}} = 0.80 \begin{bmatrix} 3000 \\ 1000 \end{bmatrix} = \begin{bmatrix} 2400 \\ 800 \end{bmatrix} \qquad (C7)$$

is $R(0.80) \approx 0.64$. Thus, if many such panels are involved, approximately 64 percent of them survive at this load level.

Based on the same approach described above, a histogram that indicates the frequency distribution of F can be generated. For example, the approach used to calculate the probability that the panel will fail in the range $0.80 \leq F \leq 0.85$ is illustrated in figures C2(c) and C2(d). The sum of the areas of the two shaded regions gives the desired probability.

The intersections occur at

$$\left. \begin{array}{l} e_1 = -0.01739 \\ e_2 = -0.009696 \\ e_3 = 0.1092 \\ e_4 = 0.1660 \end{array} \right\} \qquad (C8)$$

The corresponding standardized variables are calculated to be

$$\left.\begin{array}{l} \overline{e}_1 = -0.3478 \\[4pt] \overline{e}_2 = -0.1939 \\[4pt] \overline{e}_3 = 2.184 \\[4pt] \overline{e}_4 = 3.320 \end{array}\right\} \qquad (C9)$$

The total shaded area A is given by

$$A = \Phi\left(\overline{e}_2\right) - \Phi\left(\overline{e}_1\right) + \Phi\left(\overline{e}_4\right) - \Phi\left(\overline{e}_3\right)$$

$$= 0.42313 - 0.36400 + 0.99955 - 0.98552$$

$$= 0.07316 \qquad (C10)$$

Thus, approximately 7.3 percent of these panels fail in the range $0.80 \leq F \leq 0.85$. An alternate way to interpret the above calculation is to note that $P(0.80 \leq F \leq 0.85) = R(0.80) - R(0.85)$.

This approach can also be used to calculate the probability density function for failure. The probability density is given (in this case) by $-\partial R/\partial F$, which can be evaluated with the finite difference approximation $-\Delta R/\Delta F$. The quantity ΔR is the change in R between two values of F and is given by equation (C10) with a change in sign. The quantity ΔF is the increment in F used to calculate ΔR. By using the data in the previous example, we can approximate the probability density of F at $F = 0.825$ (the midpoint of the increment) with

$$-\frac{\Delta R}{\Delta F} = -\frac{-0.07316}{0.05} \approx 1.46 \qquad (C11)$$

Appendix D

Distribution Functions and Related Statistical Parameters

The symbol F is the traditional symbol used to denote the cumulative distribution function. That is the way it is used in this appendix, but in this appendix only. In all other portions of this report, the symbol F has a different meaning, as noted in the list of symbols. Additional information on the distributions summarized in this appendix is given in references 24–28, 31, and 32.

Normal Distribution

The two parameters of this distribution are μ and σ, where $\sigma > 0$.

For the cumulative distribution function,

$$F(x) = \frac{1}{\sigma\sqrt{2\pi}} \int_{-\infty}^{x} \exp\left[-(t-\mu)^2/2\sigma^2\right] dt \qquad (-\infty < x < \infty) \tag{D1}$$

For the probability density function,

$$f(x) = \frac{1}{\sigma\sqrt{2\pi}} \exp\left[-(x-\mu)^2/2\sigma^2\right] \qquad (-\infty < x < \infty) \tag{D2}$$

Mean = Mode = Median = μ

Standard deviation = σ

For a standard normal distribution, substitute $z = (x-\mu)/\sigma$ into equations (D1) and (D2). Note that in equations (D1) and (D3), t is a dummy variable.

For the standard cumulative distribution function,

$$\Phi(z) = F(z) = \frac{1}{\sqrt{2\pi}} \int_{-\infty}^{z} \exp\left(-t^2/2\right) dt \qquad (-\infty < z < \infty) \tag{D3}$$

For the standard probability density function,

$$\phi(z) = f(z) = \frac{1}{\sqrt{2\pi}} \exp\left(-z^2/2\right) \qquad (-\infty < z < \infty) \tag{D4}$$

Mean = Mode = Median = 0

Standard deviation = 1

Type I Asymptotic Distribution of Maximum Extreme Values

The two parameters of the distribution are u and a, where $a > 0$.

For the cumulative distribution function,

$$F(x) = \exp\{-\exp[-a(x-u)]\} \qquad (-\infty < x < \infty) \tag{D5}$$

For the probability density function,

$$f(x) = a \exp\{-a(x-u) - \exp[-a(x-u)]\} \qquad (-\infty < x < \infty) \qquad \text{(D6)}$$

$$\text{Mean} \approx \frac{u + 0.5772}{a} \qquad\qquad (0.5772 \text{ is Euler's constant})$$

$$\text{Mode} = u$$

$$\text{Median} = \frac{u - [\ln(\ln 2)]}{a}$$

$$\text{Standard deviation} = \frac{\pi}{a\sqrt{6}} \approx \frac{1.2825}{a}$$

Type I Asymptotic Distribution of Minimum Extreme Values

The two parameters of the distribution are u and a, where $a > 0$.

For the cumulative distribution function,

$$F(x) = 1 - \exp\{-\exp[a(x-u)]\} \qquad (-\infty < x < \infty) \qquad \text{(D7)}$$

For the probability density function,

$$f(x) = a \exp\{a(x-u) - \exp[a(x-u)]\} \qquad (-\infty < x < \infty) \qquad \text{(D8)}$$

$$\text{Mean} \approx \frac{u - 0.5772}{a} \qquad\qquad (0.5772 \text{ is Euler's constant})$$

$$\text{Mode} = u$$

$$\text{Median} = \frac{u + [\ln(\ln 2)]}{a}$$

$$\text{Standard deviation} = \frac{\pi}{a\sqrt{6}} \approx \frac{1.2825}{a}$$

Truncated Distributions

The truncated distributions used in this report are similar to the original distributions with two exceptions. First, the tails of each probability density function (pdf) are eliminated. Second, the remaining portion of each pdf is multiplied by a factor greater than unity to account for the "missing" tails. The factor is the reciprocal of the area under the remaining pdf. As a result, the area under the pdf of the truncated distribution is equal to unity. The cumulative distribution function is adjusted with the same factor.

For example, in the case of the truncated normal distribution with the truncation at $\pm 2\sigma$, the factor is approximately 1.0477. The pdf is given by

$$f(x) = \begin{cases} 0 & (x < -2\sigma) \\ \frac{1.0477}{\sigma\sqrt{2\pi}} \exp\left[-(x-u)^2/2\sigma^2\right] & (-2\sigma \leq x \leq 2\sigma) \\ 0 & (x > 2\sigma) \end{cases} \qquad \text{(D9)}$$

For the two extreme value distributions, the factor is approximately 1.0449. The pdf's for the original and truncated distributions are shown in figure D1.
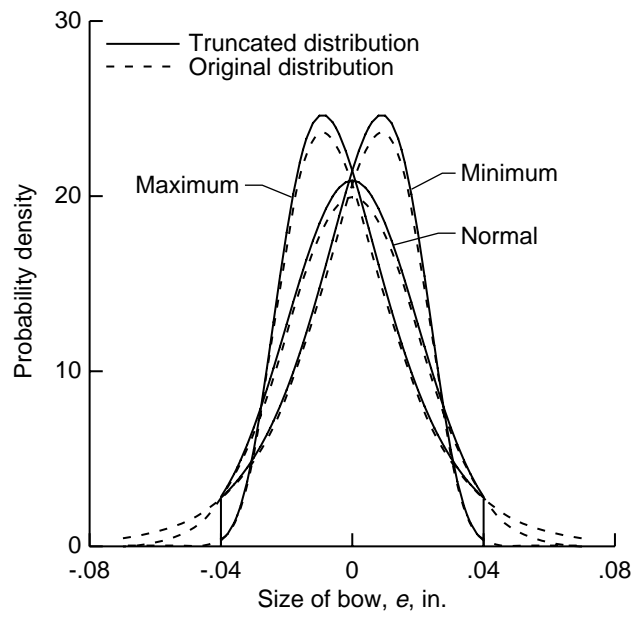
20

Figure D1. Probability density functions for distributions shown in figures 15 and 18.

References

1. Donnell, L. H.; and Wan, C. C.: Effect of Imperfections on Buckling of Thin Cylinders and Columns Under Axial Compression. *J. Appl. Mech.,* vol. 17, no. 1, Mar. 1950, pp. 73–83.

2. Babcock, C. D.; and Sechler, E. E.: *The Effect of Initial Imperfections on the Buckling Stress of Cylindrical Shells.* NASA TN D-2005, 1963.

3. Hutchinson, J. W.; and Koiter, W. T.: Postbuckling Theory. *Appl. Mech. Reviews,* vol. 23, no. 12, Dec. 1970, pp. 1353–1366.

4. Arbocz, J.; and Sechler, E. E.: On the Buckling of Axially Compressed Imperfect Cylindrical Shells. *Trans. ASME: J. Appl. Mech.,* vol. 41, ser. E, no. 3, Sept. 1974, pp. 737–743.

5. Budiansky, B.; and Hutchinson, J. W.: Buckling—Progress and Challenge. *Trends in Solid Mechanics 1979—Proceedings of the Symposium Dedicated to the 65th Birthday of W. T. Koiter,* J. F. Besseling and A. M. A. Van der Heijden, eds., Delft Univ. Press (Netherlands), 1979, pp. 185–208.

6. Thompson, J. M. T.; and Hunt, G. W.: *A General Theory of Elastic Stability.* John Wiley & Sons, c.1973.

7. Elishakoff, Isaac; and Arbocz, Johann: Reliability of Axially Compressed Cylindrical Shells With General Non-symmetric Imperfections. *Trans. ASME: J. Appl. Mech.,* vol. 52, no. 1, Mar. 1985, pp. 122–128.

8. Elishakoff, I.; Van Manen, S.; Vermeulen, P. G.; and Arbocz, J.: First-Order Second-Moment Analysis of the Buckling of Shells With Random Imperfections. *AIAA J.,* vol. 25, no. 8, Aug. 1987, pp. 1113–1117.

9. Arbocz, J.; and Hol, J. M. A. M.: *Recent Development in Shell Stability Analysis.* Rep. LR-633, Faculty of Aerospace Engineering, Delft Univ. of Technology, May 1990.

10. Giles, Gary L.; and Anderson, Melvin S.: *Effects of Eccentricities and Lateral Pressure on the Design of Stiffened Compression Panels.* NASA TN D-6784, 1972.

11. Stroud, W. Jefferson; Anderson, Melvin S.; and Hennessy, Katherine W.: *Effect of Bow-Type Initial Imperfection on the Buckling Load and Mass of Graphite-Epoxy Blade-Stiffened Panels.* NASA TM-74063, 1977.

12. Anderson, Melvin S.; and Stroud, W. Jefferson: A General Panel Sizing Computer Code and Its Application to Composite Structural Panels. *AIAA J.,* vol. 17, no. 8, Aug. 1979, pp. 892–897.

13. Stroud, W. Jefferson; and Anderson, Melvin S.: PASCO: *Structural Panel Analysis and Sizing Code, Capability and Analytical Foundations.* NASA TM-80181, 1981. (Supersedes NASA TM-80181, 1980.)

14. Anderson, Melvin S.; Stroud, W. Jefferson; Durling, Barbara J.; and Hennessy, Katherine W.: *PASCO: Structural Panel Analysis and Sizing Code, User's Manual.* NASA TM-80182, 1981. (Supersedes NASA TM-80182, 1980.)

15. Stroud, W. J.: Optimization of Composite Structures. *Mechanics of Composite Materials—Recent Advances,* Zvi Hashin and Carl T. Herakovich, eds., Pergamon Press, Inc., c.1983, pp. 307–322.

16. Stroud, W. Jefferson; Greene, William H.; and Anderson, Melvin S.: *Buckling Loads of Stiffened Panels Subjected to Combined Longitudinal Compression and Shear: Results Obtained With PASCO, EAL, and STAGS Computer Programs.* NASA TP-2215, 1984.

17. Wittrick, W. H.; and Williams, F. W.: Buckling and Vibration of Anisotropic or Isotropic Plate Assemblies Under Combined Loadings. *Int. J. Mech. Sci.,* vol. 16, no. 4, Apr. 1974, pp. 209–239.

18. Williams, F. W.; and Anderson, M. E.: *User's Guide to VIPASA (Vibration and Instability of Plate Assemblies Including Shear and Anisotropy).* Dep. of Civil Engineering, Univ. of Birmingham, England, Jan. 1973.

19. Anderson, Melvin S.; Hennessy, Katherine W.; and Heard, Walter, L., Jr.: *Addendum to Users Guide to VIPASA (Vibration and Instability of Plate Assemblies Including Shear and Anisotropy).* NASA TM X-73914, 1976.

20. Anderson, M. S.; Williams, F. W.; and Wright, C. J.: Buckling and Vibration of Any Prismatic Assembly of Shear and Compression Loaded Anisotropic Plates With an Arbitrary Supporting Structure. *Int. J. Mech. Sci.,* vol. 25, no. 8, 1983, pp. 585–596.

21. Williams, F. W.; Kennedy, D.; and Anderson, M. S.: Analysis Features of VICONOPT, an Exact Buckling and Vibration Program for Prismatic Assemblies of Anisotropic Plates. *A Collection of Technical Papers, Part 2—AIAA/ASME/ASCE/AHS/ASC 31st Structures, Structural Dynamics and Materials Conference,* Apr. 1990, pp. 920–929. (Available as AIAA-90-0970-CP.)

22. Butler, R.; and Williams, F. W.: Optimum Design Features of VICONOPT, an Exact Buckling Program for Prismatic Assemblies of Anisotropic Plates. *A Collection of Technical Papers, Part 2—AIAA/ASME/ASCE/AHS/ASC 31st Structures, Structural Dynamics and Materials Conference,* Apr. 1990, pp. 1289–1299. (Available as AIAA-90-1068-CP.)

23. Williams, F. W.; Anderson, M. S.; Kennedy, D.; Butler, R.; and Aston, G.: *User Manual for VICONOPT—An Exact Analysis and Optimum Design Program Covering the Buckling and Vibration of Prismatic Assemblies of Flat In-Plane Loaded, Anisotropic Plates, With Approximations for Discrete Supports and Transverse Stiffeners.* NASA CR-181966, 1990.

24. Elishakoff, Isaac: *Probabilistic Methods in the Theory of Structures.* John Wiley & Sons, Inc., c.1983.

25. Ang, Alfredo H-S; and Tang, Wilson H.: *Probability Concepts in Engineering Planning and Design. Volume I—Basic Principles.* John Wiley & Sons, Inc., c.1975.

26. Benjamin, Jack R.; and Cornell, C. Allin: *Probability Statistics, and Decision for Civil Engineers.* McGraw-Hill Inc., c.1970.

27. Soong, T. T.: *Probabilistic Modeling and Analysis in Science and Engineering.* John Wiley & Sons, Inc., c.1981.

28. Ang, Alfredo H-S; and Tang, Wilson H.: *Probability Concepts in Engineering Planning and Design. Volume II—Decision, Risk, and Reliability.* John Wiley & Sons, Inc., c.1984.

29. Vanderplaats, Garret N.: *CONMIN—A FORTRAN Program for Constrained Function Minimization, User's Manual.* NASA TM X-62282, 1973.

30. Vanderplaats, Garret N.; and Moses, Fred: Structural Optimization by Methods of Feasible Directions. *Int. J. Computers & Struct.,* vol. 3, no. 4, July 1973, pp. 739–755.

31. Leporati, Ezio (Nicoletta Grimoldi, transl.): *The Assessment of Structural Safety. Volume 1 of Series in Cement and Concrete Research,* Andrew Short, ed., Research Studies Press, c.1979.

32. Madsen, H. O.; Krenk, S.; and Lind, N. C.: *Methods of Structural Safety.* Prentice-Hall, Inc., c.1986.

REPORT DOCUMENTATION PAGE

1. AGENCY USE ONLY (Leave blank)	2. REPORT DATE January 1993	3. REPORT TYPE AND DATES COVERED Technical Paper

4. TITLE AND SUBTITLE
Effect of Bow-Type Initial Imperfection on Reliability of Minimum-Weight, Stiffened Structural Panels

5. FUNDING NUMBERS
WU 505-63-53-01

6. AUTHOR(S)
W. Jefferson Stroud, Thiagaraja Krishnamurthy, Nancy P. Sykes, and Isaac Elishakoff

7. PERFORMING ORGANIZATION NAME(S) AND ADDRESS(ES)
NASA Langley Research Center
Hampton, VA 23681-0001

8. PERFORMING ORGANIZATION REPORT NUMBER
L-17089

9. SPONSORING/MONITORING AGENCY NAME(S) AND ADDRESS(ES)
National Aeronautics and Space Administration
Washington, DC 20546-0001

10. SPONSORING/MONITORING AGENCY REPORT NUMBER
NASA TP-3263

11. SUPPLEMENTARY NOTES
Stroud: NASA Langley Research Center, Hampton, Virginia; Krishnamurthy and Sykes: Analytical Services & Materials, Inc., Hampton, Virginia; Elishakoff: Florida Atlantic University, Boca Raton, Florida.

12a. DISTRIBUTION/AVAILABILITY STATEMENT

Unclassified–Unlimited

Subject Category 39

12b. DISTRIBUTION CODE

13. ABSTRACT (Maximum 200 words)
Computations were performed to determine the effect of an overall bow-type imperfection on the reliability of structural panels under combined compression and shear loadings. A panel's reliability is the probability that it will perform the intended function—in this case, carry a given load without buckling or exceeding in-plane strain allowables. For a panel loaded in compression, a small initial bow can cause large bending stresses that reduce both the buckling load and the load at which strain allowables are exceeded; hence, the bow reduces the reliability of the panel. In this report, analytical studies on two stiffened panels quantified that effect. The bow is in the shape of a half-sine wave along the length of the panel. The size e of the bow at panel midlength is taken to be the single random variable. Several probability density distributions for e are examined to determine the sensitivity of the reliability to details of the bow statistics. In addition, the effects of quality control are explored with truncated distributions.

14. SUBJECT TERMS
Reliability; Imperfections; Stiffened panels; Buckling; Probabilistic analysis

15. NUMBER OF PAGES
26

16. PRICE CODE
A03

17. SECURITY CLASSIFICATION OF REPORT Unclassified	18. SECURITY CLASSIFICATION OF THIS PAGE Unclassified	19. SECURITY CLASSIFICATION OF ABSTRACT	20. LIMITATION OF ABSTRACT